Analytical and Bioanalytical Chemistry (2018) 410:3161–3170
https://doi.org/10.1007/s00216-018-1003-0

RESEARCH PAPER

Highly sensitive detection of a small molecule by a paired labels recognition system based lateral flow assay

Leina Dou[1] · Bingxin Zhao[1] · Tong Bu[1] · Wentao Zhang[1] · Qiong Huang[1] · Lingzhi Yan[1] · Lunjie Huang[1] · Yanru Wang[1] · Jianlong Wang[1] · Daohong Zhang[1]

Received: 25 December 2017 / Revised: 19 February 2018 / Accepted: 6 March 2018 / Published online: 28 March 2018

Abstract

Small molecules are difficult to detect by conventional gold lateral flow assay (GLFA) sensitively because the test system must satisfy the conflict requirements between enough signal intensity and limited antibody (Ab) amount. In this work, a paired labels recognition (PLR)-based biosensor was designed by utilizing the specific binding of Ab and secondary antibody (anti-Ab) to enhance signal intensity and reduce antibody amount applied in small molecule detection. The PLR amplification system is fabricated by self-assembling the common detection probe, Au-labeled Ab (Au-Ab), and the signal booster, Au-labeled anti-Ab (Au-anti-Ab). Benefiting from this, a powerful network structure can be generated to accumulate numerous gold nanoparticles (GNPs) and thus significantly strengthen the signal intensity of detection. Therefore, a lower Ab amount will be applied to offer adequate signal strength, and further, the limit of detection will be obviously downregulated due to the more effective competition reaction. Using furazolidone (FZD) as a model analyte, we achieve a detection limit of as low as 1 ng mL^{-1}, which was at least fivefold improved over that of the traditional GLFA. Furthermore, the practicality of this strategy was certificated in five different food samples.

Keywords Lateral flow assay · Gold nanoparticles · Signal amplification · Furazolidone · Food analysis

Introduction

Gold lateral flow assay which enables an easy-to-operate, fast-response, and cost-effective detection of target analyte is a classical and most widely used commercial technical method for point-of-care testing [1]. Being very simple to apply, such test strips have received tremendous attention in areas ranging from disease diagnosis [2–4] and environmental monitoring [5] to food quality control [6, 7]. Gold lateral flow assay (GLFA) with competitive format has been extensively applied to detect small chemical molecules with lower molecular weight and single antigenic determinants [8]. However, low bright intensity of conventional gold nanoparticle (GNP)-based competitive LFA results in a poor sensitivity for analyte, which constraints its further applications in some cases requiring high sensitivity [9]. Additionally, for competitive analyses in which an inverse relationship exists between the assay sensitivity and the detectable signal, although low signal intensity can give a relatively higher sensitivity, poor observability and decreased accuracy will also follow. On the other hand, it is difficult to achieve enhanced signal intensity and simple manipulation simultaneously [10–12]. Therefore, to fulfill the requirements of both high-sensitive and simple manipulation at the signal amplification based GLFA is becoming increasingly important.

Hitherto, compared to sandwich GLFAs [13–15], the signal-amplified competitive GLFA as a bio-platform for small molecule management is still largely unexplored. Thereinto, the efficient efforts that have been made to ameliorate the performance of competitive GLFA are the so-called sliver enhancement. For example, in 2010, Liao et al. prepared a silver core and a gold shell nanoparticle to detect aflatoxin B_1 [16]. More recently, Baggiani et al. exploited the same principle to detect ochratoxin A [17]. Although silver enhancement can be

Electronic supplementary material The online version of this article (https://doi.org/10.1007/s00216-018-1003-0) contains supplementary material, which is available to authorized users.

✉ Daohong Zhang
zhangdh@nwsuaf.edu.cn

[1] College of Food Science and Engineering, Northwest A&F University, Yangling, Shaanxi 712100, China

used as a generic approach to improve the GLFA systems, the visible color is mainly derived from the reinforcement after the immunological chromatography reaction in the test (T) line, which was often uncontrollable. Besides, development of the silver metal also requires additional manual procedures and incubation time, which makes the immunochromatographic technique more complex and time-consuming [18]. Thus, it is still imperative to construct a more effective signal-amplified competitive GLFA to conquer the contradiction between signal intensity enhancement and operational complexity for small molecule detection using minimum consumption of antibody.

With this motivation, we exploit a PLR system-based signal amplification GLFA format for visual determination of small molecules. The mechanism of the proposed strategy is based on the specific recognition of Ab and anti-Ab. During the chromatographic process, a PLR system was fabricated by self-assembling the detection probe of Au-Ab and a signal booster of Au-anti-Ab. In the T-line, the signal was enriched following the forming of signal network structure with abundant GNPs accumulated on T-line. Thereby, compared to the conventional competitive GLFA in which only Au-Ab is used to offer signal, fewer Abs (detection probes) were needed to produce clearly visible results. Then, the further decreasing Ab would trigger more intensified competition between free analyte and the immobilized antigen (Ag) for limited Ag combining sites, bringing more sensitive concentration-response relation between the analyte and signal intensity. Besides, the two compounds were first dispensed onto the same one conjugate pad in sequences. Benefiting from this, the method can accomplish detection and signal amplification at the same time without any additional reagents and manipulations. Furazolidone (FZD) was chosen as the example of a monitoring target. FZD is a kind of nitrofuran antibiotics which are used to prevent and treat gastrointestinal infections and other diseases caused by *Escherichia coli* or *Salmonella*. Due to the short half-life, the FZD parent drug is extremely unstable in vivo, while its metabolite, 3-amino-2-oxazolidinone (AOZ), is highly stable in tissue matrices, becoming the residual marker for FZD residual monitoring. Considering the potential carcinogenicity and mutagenicity of its residue in edible tissues, the usage of FZD has been forbidden in food-producing animals by the European Union, the USA, and China. In spite of this, driven by economic interests, nitrofurans are still illegally abused by many livestock, poultry, and aquaculture manufacturers, owing to its excellent curative effects, resulting in a tremendous threat to human health [19–23]. Furthermore, the feasibility of this strategy was testified by AOZ detection in five different food samples (milk power, shrimp, chicken, fish, and pork).

Experimental

Reagents and materials

AOZ, 3-[(4-carboxyphenyl) monomethyl] amino-2-oxazolidinone (CPAOZ), CPAHD, CPSEM, CPAMOZ, lexdopamine, salbutamol, clenbuterol, chloramphenicol, and penicillin were purchased from Anti Biotechnology (Wuhan, China). High specific monoclonal antibody against CPAOZ was prepared in our laboratory. Anti-Ab (goat anti-mouse IgG) was received from Luoyang Baiaotong Experimental Materials Center (Luoyang, China, http://kangyuangkangti.cn.makepolo.com/). Hydrogen tetrachloroaurate (III) hydrate ($HAuCl_4 \cdot 3H_2O$), bovine serum albumin (BSA), 4-carboxybenzaldehyde (4-CBA), and dimethyl sulfoxide were obtained from Sigma-Aldrich (USA, http://www.sigmaaldrich.com/china-mainland.html). Milk power, shrimp, chicken, fish, and pork were purchased from a local supermarket in Yangling, China. Nitrocellulose (NC) membranes were prepared from Millipore Corp (Shanghai, China, http://www.merckmillipore.com/). All solvents and other chemicals were of analytical grade and used as received. Ultrapure water (18.2 MΩ cm) produced by a Milli-Q system was used throughout this work.

Apparatus

Guillotine cutter (HGS-201) and dispensing platform (HGS510-2D) were used to prepare test strips which were received from Hangzhou Autokun Technology Co., Ltd. (Hangzhou, China, http://www.autokun.com/). The high-speed refrigerated centrifuge (HC-3018R) was obtained from Anhui USTC Zonkia Scientific Instruments Co., Ltd. (Anhui, China, http://www.zonkia.com.cn/). Vacuum freeze dryer (FDS-2.5E) was purchased from SIM International Group Co., Ltd. (Beijing, China, https://simcsales.en.ec21.com/).

Preparation of GNPs

GNPs with average diameter of 15 nm were synthesized as the classical method [24] with slight modifications. All glassware used in the process were soaked with aqua regia (HCl/HNO_3) for more than 2 h. Briefly, 1 mL of 1% $HAuCl_4 \cdot 3H_2O$ was added into 96 mL ultra-pure water, stirred, and heated to boiling point. And 4 mL of 1% trisodium citrate was added rapidly with vigorous stirring. The mixture was churned continuously until the color turned to red, then the compound was boiled for another 10 min to ensure a stable color. After cooling to room temperature, a certain volume of ultra-pure water was added to the solution to restore the original volume, and the final product was kept at 4 °C for subsequent usage.

Preparations of Au-Ab and Au-anti-Ab composites

The Au-Ab was synthesized by the previously established method [25]. The pH of the GNPs was adjusted by adding 0.01 M K_2CO_3 before the addition of Ab. And the minimum amount of Ab to stabilize the GNPs was determined as preceding reports. Then the appropriate amount of Ab was added to the pH-adjusted GNP solution in a stirred state and agitated for another 30 min. Subsequently, 10% BSA solution was mixed to the compound to achieve a final concentration of 1% to block the residual binding sites on GNPs surface. The mixture was stirred for 30 min again and preserved at 4 °C for 2 h. Then the mixture was centrifuged at 1500 rpm for 15 min to remove the aggregated GNPs, and the supernatant was collected and centrifuged at 12,000 rpm for 35 min to eliminate the unconjugated Ab and BSA. Finally, the precipitation was washed with 2 mM borax buffer (pH 9.0) containing 0.1% (*w*/*v*) PEG-20000 and 0.02% sodium azide (NaN_3). The final pellet was resuspended in the borax buffer and maintained at 4 °C for further experiments.

The Au-anti-Ab was also prepared by the aforementioned process under the same conditions.

Manufacture of the traditional and novel GLFAs

In this section, blocking buffers (solutions that contain several kinds of additions, which can affect the characters of reactant flow, level of background color, signal intensity, and sensitivity of LFIA) were first prepared by adding different ingredients in ultrapure water and then mixing with a vortexer.

As illustrated in Fig. 1, the GLFA was made up of plastic plate, sample pad, conjugate release pad, NC membrane, and absorbent pad. And the fabrication process was based on four major steps: (i) the sample and conjugate pads were pretreated by soaking in blocking buffers for several minutes respectively and dried at 37 °C overnight. The absorbent pad was served as a capillary pump to draw the fluid and employed without treatment. (ii) The Au-Ab composite was dispensed onto the conjugate pad with desired volume and dried in a vacuum freeze drier for 3 h. (iii) The optimum amount of Ag and anti-Ab (1 mg mL^{-1} with a density of 1 μL cm^{-1}) were dispensed onto the suitable reaction area of the NC membrane as test and control (C) lines separately, in which the former gave information about the target analyte, while the latter ensured the correct functioning of the test [26]. The distance between the two lines was 6 mm. After that, the NC membrane was dried for 30 min at room temperature. (iv) All parts mentioned above were assembled onto a plastic adhesive backing card in order to form GLFA, which was then cut into 3 mm width using automatic programmable cutter and stored in a desiccator until use.

The PLR-based strip was assembled with a little modification on the basis of the traditional GLFA. First of all, two composites of Au-Ab and Au-anti-Ab were used and both dispensed onto the same conjugate pad at different positions, so the conjugate pad was longer than that of general GLFA (Fig. 1). Secondly, no C-line on the NC membrane as usual was dispensed.

Assay procedure and performance evaluation

Sample solutions with and without CPAOZ were separately pipetted into wells of a microtiter plate in duplicate ($n = 3$), then sample pads of strips were vertically inserted into the wells. For the performance evaluation of the novel biosensor, CPAOZ standard was diluted by 10 mM phosphate-buffered solution (PBS, pH 7.4) to a series of concentrations of 0, 0.1, 0.3, 0.5, 0.8, 1, and 3 ng mL^{-1}. Unamplified lateral flow assay used for comparison was conducted as well and the concentrations of CPAOZ were set at 0, 0.5, 1, 2, 3, 5, and 7 ng mL^{-1}. After 10 min of the reaction, the color signals were qualitatively observed by naked eyes and quantitatively analyzed by the Image J software analysis.

The cross-reactivity of the developed assay was evaluated using CPAOZ as the target analyte, followed by other structurally similar compounds of 3-nitrofuran and 5-non-nitrofuran antibiotics, including CPAHD, CPSEM, CPAMOZ and lex-dopamine, salbutamol, clenbuterol,

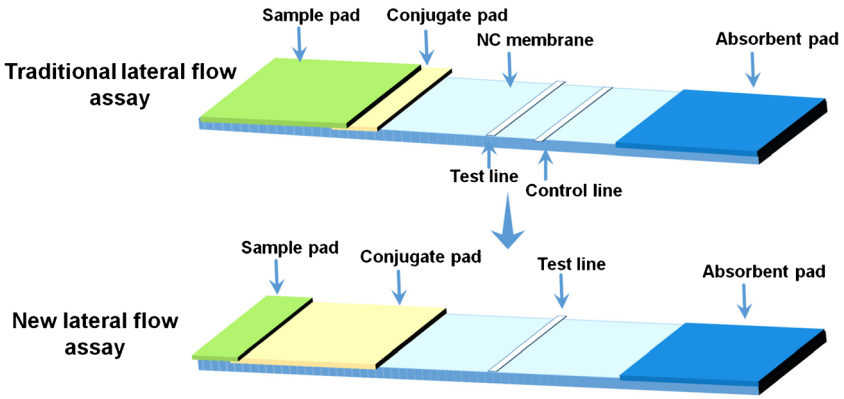

Fig. 1 Structural representations of both traditional and novel GLFAs

chloramphenicol, and penicillin, respectively as interfering compounds. Each interfering substance was individually diluted to the concentration of 100 ng mL^{-1}, while the target was diluted to 1 ng mL^{-1}, and tested by proposed GLFA to evaluate the assay specificity. The control groups were PBS buffer. All experiments were performed in triplicates.

Detection of AOZ in food samples

The applicability of this strategy was evaluated by adding AOZ standards of known concentrations to five different food samples, including milk power, shrimp, chicken, fish, and pork, which had been determined beforehand by high-performance liquid chromatography (HPLC) method to be free of AOZ. For the detection of AOZ, the sample solutions were derived with 4-CBA and the derivatization reaction is given in Fig. 2. Specifically, muscle tissues from chicken, pork, fish, and shrimp were filleted or minced, then homogenized by a mixer to form homogenates. Accurately weighted 1.0 g of homogeneous samples and milk powder were first dissolved with ultrapure water and distributed into 10-mL centrifuge tubes. Then the samples were spiked with 0–3 and 0–7 ng mL^{-1} AOZ standard solutions for traditional and novel LFIAs respectively, and the mixtures were vortexed at room temperature for a while. Then, 200 μL of 4-CBA (0.05 M) in dimethyl sulfoxide was added to the samples, and each tube was incubated at 37 °C for 16 h. Afterwards, the derived samples were centrifuged at 10,000 rpm for 10 min, the supernatants were collected and analyzed in triplicate by the new GLFA under the optimal experimental conditions. Moreover, the recovery rates of the novel GLFA obtained in blank food samples spiked with AOZ, at levels of 0.1, 0.5, and 0.8 ng mL^{-1}, and were measured using the following equation: (concentration measured/concentration spiked) × 100%. In each detection, a blank control GLFA was carried out to play a role in monitoring whether the test strip is valid or not.

Results and discussion

Principle for signal-amplified GLFA

The improved GLFA was based on the amplified signal and more effective competition reaction. The detection probe of Au-Ab and the signal booster of Au-anti-Ab together constituted the paired labels recognition system. As shown in Fig. 3a, one Au-Ab probe can bind several Au-anti-Ab boosters and then one conjugated Au-anti-Ab can combine with several Au-Ab probes again to generate a powerful network structure, then a deepening color developed on the T-line because of the accumulation of GNPs in the network. In order to verify the formation of the network structure, anti-Ab was coated as C-line in the new strips which were then used in the analysis of blank and positive samples in triplicate. As shown in Fig. 3b, weak red bands and red bands can be seen in C-lines for blank and positive tests. The result exhibited that there were unbound murine antibodies exposed outside of the network complex, which indirectly proved that the binding of two composites generated a network structure.

The GLFAs are carried out based on the migration of test solution along the Ag-immobilized test strip where the corresponding specific competitive immune recognition reaction takes place [27]. The principle of the PLR system-based GLFA is illustrated minutely in Fig. 3c. After immersing the end of the strip into the reaction cell, immediately, the sample solution migrated along the strip by capillary force. When the solution flowed into the conjugate pad, the Au-Ab and Au-anti-Ab were eluted successively and then quickly combined together before they reached the test zone. Then, for a negative test, the network-probe combination was captured on the T-line due to the reaction between immobilized CPAOZ-BSA and anti-CPAOZ Ab in Au-Ab probe. Thus, a three-dimensional signal network self-assembling from Au-Ab and Au-anti-Ab was formed and captured on T-line, resulting in a distinctive deepened red band. For the positive assay, the CPAOZ antibody-anti-antibody complex migrated directly to the absorbent pad, and no antibody-anti-antibody-GNPs marker or only a part of that marker was entrapped on NC membrane, generating no or a weaker color on the T-line. Therefore, an approximately inversely proportional relationship existed between the color intensity of T-line and the concentration of FZD metabolite in samples.

Characterization of GNPs

The GNPs used in our work were investigated and validated by three methods of UV-vis, dynamic light scattering (DLS), and high-resolution transmission electron microscopy (HRTEM). As illustrated in Fig. 4a, the UV-vis absorption

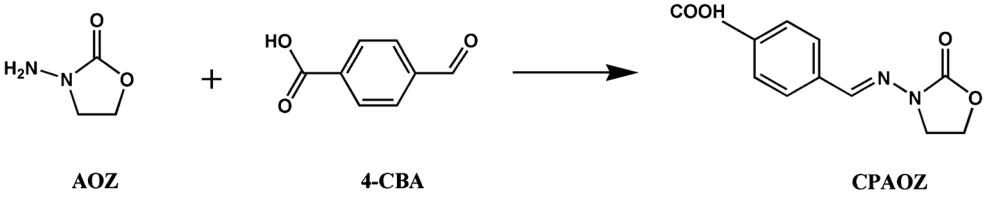

Fig. 2 Chemical structure and derivatizing reaction of AOZ

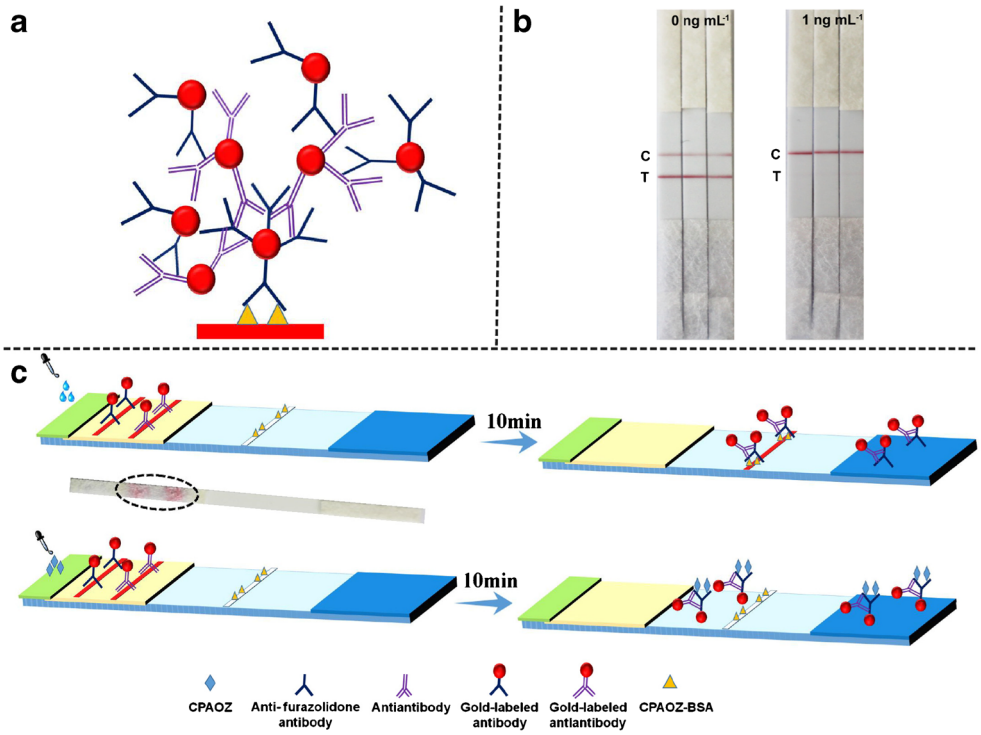

Fig. 3 Demonstration diagram of principles for signal amplification and the new GLFA. **a** Mechanism of the PLR-based signal amplifying system. **b** Assay results of the C-line dispensed new GLFA, 0 and 1 ng mL^{-1} of CPAOZ were separately used in negative and positive tests. **c** Analysis process and principle for both negative and positive samples tests by the novel GLFA

spectra of the as-prepared GNPs exhibited a sufficiently narrow size distribution with well-resolved maximum absorption of surface plasmon resonance at 520 nm. And the maximum UV-vis absorption peaks were all recorded at 520 nm for different batches of GNP solutions, indicating good reproducibility. DLS analysis in Fig. 4b revealed that the average diameter of the resultant GNPs were 15 nm. Finally, the size and morphology of the GNPs were further characterized via

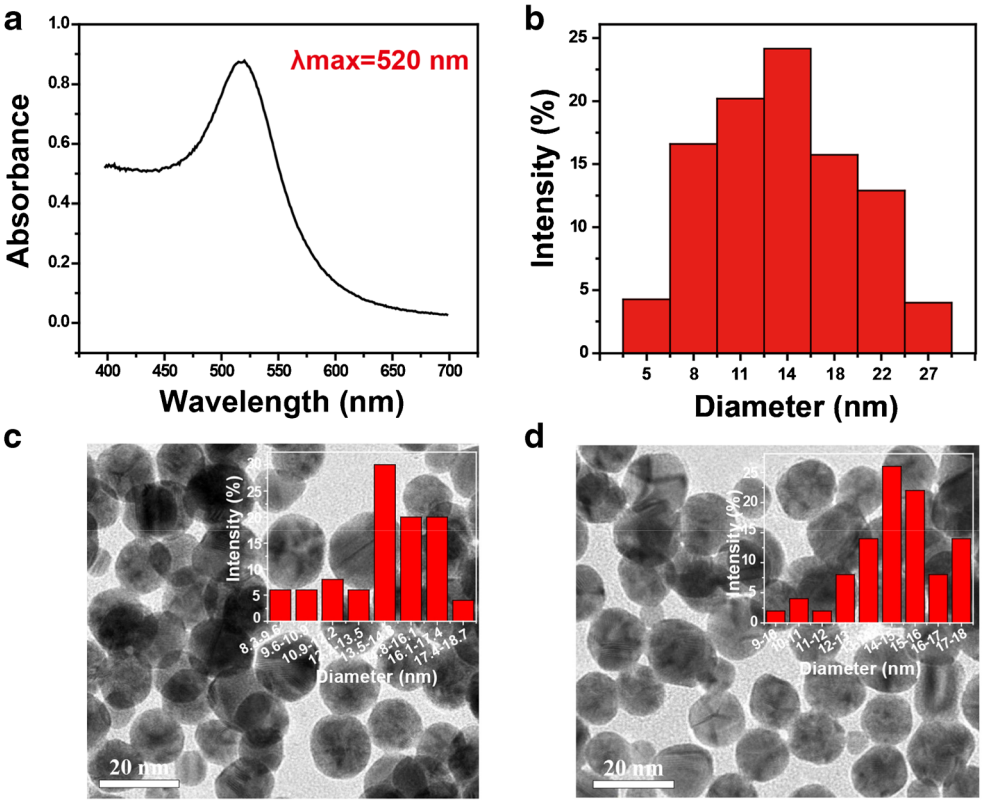

Fig. 4 Characterization of the synthetic GNPs. **a** UV-vis absorption spectrum of the GNPs solution. **b** DLS of the synthetic GNPs. **c**, **d** HRTEM micrographs of two batches of GNPs; the insets of **c** and **d** are the particle size distributions of the corresponding nanoparticles

HRTEM. Typical HRTEM images (Fig. 4c, d) collected from two batches of GNPs showed that the obtained GNPs were relatively regular. These results provided reliable signal materials for the following experiments.

Optimal dispensing conditions of the two composites

It is well-known that the amount of Ab applied on the conjugate pad is crucial in the competitive format immunoassay because it will affect the sensitivity of the assay. In the work, the applied amounts of both two composites were investigated. The dispensing rate of Au-Ab was first explored under a fixed amount of Au-anti-Ab. As depicted in Fig. 5a, the volume of the Au-Ab probe loaded on the conjugate pad have a great effect on the performance of the new GLFA. With the decrease of the Au-Ab dispensing rate from 8 to 5 μL cm^{-1}, the sensitivity is improved, but when the dispensing rate is further decreased to 3 μL cm^{-1}, false-negative results appeared on positive strip tests due to the nonspecific absorption of the redundant Au-anti-Ab composite, and, more importantly, it can only form a faint red band on the blank control test strip which is unfavorable for the observation by unaided eye. Thus, the optimal dispensing rate of the Au-Ab probe on the conjugate pad is set at 5 μL cm^{-1}.

As a signal booster, the appropriate application amount of Au-anti-Ab is also critical for the improvement of assay sensitivity, decrease of nonspecific adsorption, and elimination of background color on NC membrane. Different dispensing rates of Au-anti-Ab were estimated, as revealed in Fig. 5b, and the highest sensitivity with no background interference and no false-negative result is achieved at the dispensing rate of 6 μL cm^{-1}.

To immobilize the paired labels onto the conjugate pad, complex and direct immobilizing methods were separately implemented and compared to evaluate the difference in the assay efficiency. The former method was to mix and then incubate Au-Ab and Au-anti-Ab for a while beforehand and finally dispense the reaction complex of the paired labels onto the conjugate pad. The latter was to directly dispense Au-Ab and Au-anti-Ab separately onto the conjugate pad. As shown in Fig. S1, the assay performance of two kinds of strips separately prepared by two immobilizing methods basically had no significant difference, which maybe caused owing to the rapid recognition between Ab and anti-Ab. So, to save time and simplify manipulations, the direct immobilizing method was chosen. Meanwhile, in the direct immobilizing methods, the position influence of Au-Ab and Au-anti-Ab on the conjugate pad was also investigated. The result indicated that there was no significant relationship between the sensitivity and the sequential order of the two composites. The possible reason was that Au-Ab and Au-anti-Ab would closely combine together as soon as they were redissolved by the test solution.

Optimization of other assay conditions

To save analysis time, enhance color intensity, and improve sensitivity, blocking buffers for sample and conjugate pads, coating concentration of CPAOZ-BSA, and other experimental parameters were systematically optimized. It was known that under the premise of a clear, red color developed on T-line for negative test, the minimum consumption of CPAOZ-BSA should be used to ensure effective competition and reduce costs. As a result, 0.2 μL cm^{-1} of CPAOZ-BSA (less than the most previous GLFAs) was dispensed on the T-line and used for the following research. Furthermore, the blocking solutions for sample and conjugate pads were examined, because they may have an effect on reactant flow rate of test

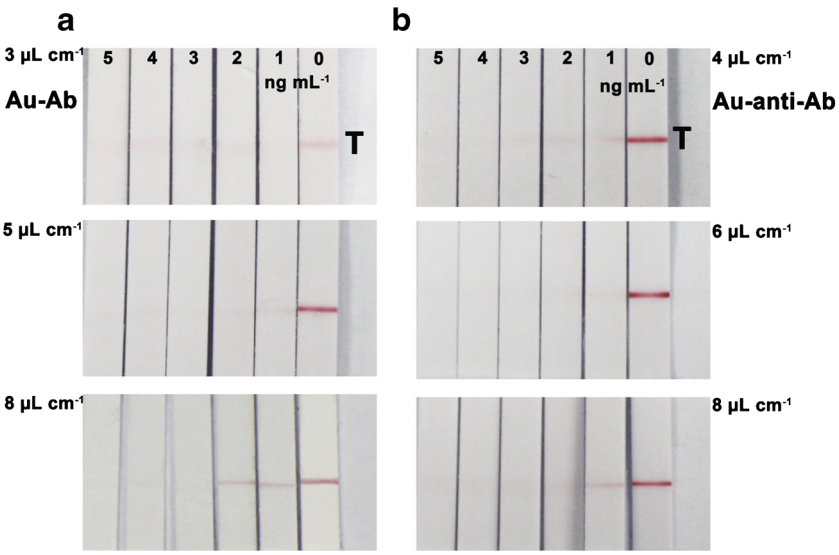

Fig. 5 Results of the PLR-based GLFA with different dispensing rates of Au-Ab and Au-anti-Ab. In both sub-pictures of **a** and **b**, from right to left 0, 1, 2, 3, 4, and 5 ng mL^{-1} of CPAOZ are used. "T" stands for test line, on which CPAOZ-BSA was immobilized

solutions, level of background color, signal generation, and sensitivity of the assay. The effects are usually caused by the components contained in the buffer, e.g., protein and polysaccharide, can block the unoccupied sites on NC membrane, and accelerate the release speed of probe from conjugate pad. In the meantime, surfactant, such as PVP-K30, not only can avoid nonspecific adsorption but also can stabilize the GNPs [28]. Moreover, the sample pad can also be impregnated with viscosity enhancers to influence the flow rate of the test solution and thus to increase the reaction time of free analyte and Ab at conjugate pad [29]. In this assay, NaN_3 was also added in a proportion of 0.02% to preserve the blocking solution for a long time. The remaining optimal assay conditions are shown in Table 1.

Performance evaluation

Before we moved onto further evaluation and application experiments, the characteristic of FZD should be carefully accessed. Due to the short half-life, the FZD parent drug is extremely unstable in vivo, while its metabolite, AOZ, is highly stable in tissue matrices. So, in the monitoring of FZD residual levels, AOZ was detected as the residual marker with its derivative of CPAOZ as the target analyte. Under optimized analysis conditions, the sensitivity of the one-step PLR system-based GLFA was investigated. Different concentrations (0–7 and 0–3 ng mL^{-1}) of CPAOZ standard in PBS buffer were simultaneously analyzed using lateral flow biosensors without and with enhancement protocols. Each sample was assayed at least three times ($n \geq 3$) and the color on the T-line was observed by bare eye in 10 min. As shown in Fig. 5, the conjugate pad of the new strip is obviously longer than that of the conventional strip, and the sensitivity of the traditional strip test is 5 ng mL^{-1} (Fig. 6a), which is determined as the minimum CPAOZ concentration that can completely inhibit the color development on T-line. While, the sensitivity of the signal-amplified GLFA is 1 ng mL^{-1} (Fig. 6b), which is at least fivefold improved than that of the traditional strip test. The results of GLFAs were further confirmed by recording the corresponding optical density values of the red bands on the test zones with Image J. From the calibration curve, it can be seen that the test line intensity is inversely correlated to the amount of CPAOZ with a good linear relationship and a correlation coefficient of 0.985 (see Electronic Supplementary Material (ESM) Fig. S2). Furthermore, according to the calibration curve, the limit of detection (LOD) and limit of quantitation (LOQ) of the PLR system-based LFIA for CPAOZ detection were calculated to be 0.13 and 0.42 ng mL^{-1}, respectively [30, 31]. Moreover, our method can compete with, or even surpass, certain two other lateral flow assays for FZD detection (see ESM Table S1).

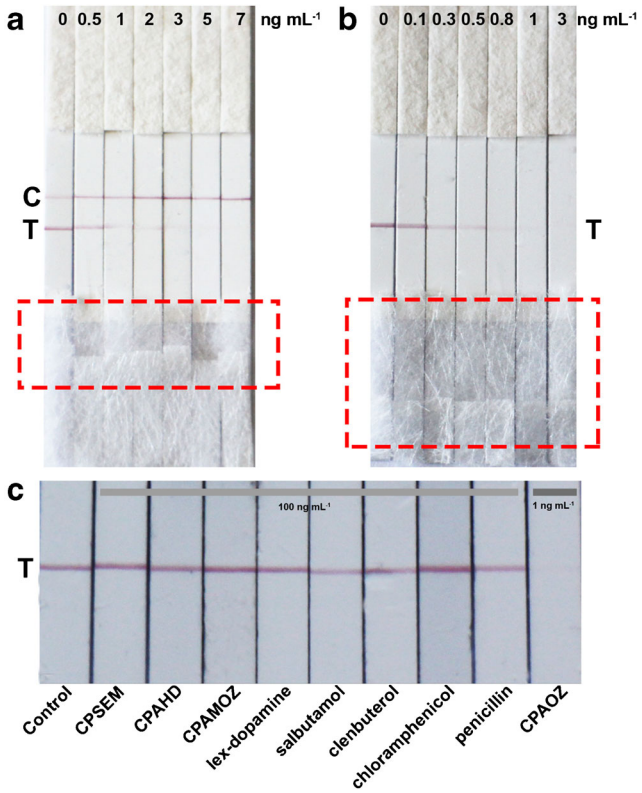

Fig. 6 Sensitivity and specificity determinations of the PLR-based GLFA for CPAOZ detection. **a**, **b** The assay results of the traditional and improved lateral flow biosensors. **c** Specificity research results of the PLR-based GLFA, in which the concentration of CPAOZ is 1 ng mL^{-1}; the concentrations of CPSEM, CPAHD, CPAMOZ, lex-dopamine, salbutamol, clenbuterol, chloramphenicol, and penicillin are all 100 ng mL^{-1}. "C" stands for control line, on which antiantibody was immobilized; "T" stands for test line, on which CPAOZ-BSA was immobilized

Furthermore, it is noteworthy that AOZ is the residual tracer of FZD in actual food samples; therefore, the

Table 1 Optimal assay conditions for the new developed GLFA

Item	Composition and concentration
Blocking buffer for conjugate pad	3% BSA, 4% sucrose, 1% PVP-K30, 0.025% Tween-20, 0.5% PEG-20000, and 0.02% NaN_3 in ultrapure water
Blocking buffer for sample pad	3% BSA, 3% sucrose, 2.5% PVP-K30, 1% PEG-20000, and 0.02% NaN_3 in ultrapure water
Coating buffer of test line	0.5 mg mL^{-1} of CPAOZ-BSA in PBS

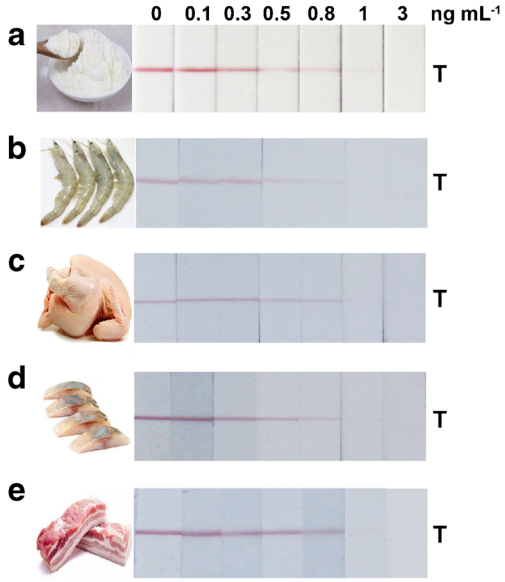

Fig. 7 Results of AOZ detection by the PLR system-based GLFA in food samples. **a**–**e** Detections in milk power, shrimp, chicken, fish, and pork samples. The numbers from left to right denote the theoretical contents (ng mL^{-1}) of CPAOZ in tested food solutions. "T" stands for test line, on which CPAOZ-BSA was immobilized

concentration of AOZ is speculated by CPAOZ using the formula mentioned below [32].

Concentration of AOZ

= (molecular weight of AOZ/molecular weight of CPAOZ)

× concentration of CPAOZ

The molecular weights of AOZ ($C_3H_6N_2O_2$) and CPAOZ ($C_{11}H_{10}N_2O_4$) are 102.11 and 234.21, respectively. According to the formula, the sensitivity of AOZ is 0.44 ng mL^{-1} for the new GLFA. It is obvious that our amplification method promised a relatively high sensitivity without complex implement and robust readout device.

To validate the specificity of this assay for CPAOZ detection, CPSEM, CPAHD, CPAMOZ, lex-dopamine, salbutamol, clenbuterol, chloramphenicol, and penicillin were used as interfering substances. The detection results are demonstrated in Fig. 6c; in the presence of only 1 ng mL^{-1} of CPAOZ, the red band on the test zone can be inhibited obviously. However, even under 100 ng mL^{-1} of other structurally similar compounds, no evident change was observed on these T-lines. Altogether, these results indicate that this method can detect CPAOZ successfully without interference from other constituents, which can be ascribed to the excellent recognition specificity of the adopted anti-CPAOZ antibody. Moreover, compared with other signal enhanced reports, the PLR system-based amplification method can obviously simplify the analysis patterns, realize one-step detection and signal amplification simultaneously, save time, and reduce costs. More significantly, it is hopeful to generalize this strategy in detections of a wide spectrum of small molecules using different antibodies.

Application of the new GLFA in food samples

An excellent applicability is necessary and significant for a newly designed sensing system. To evaluate the practical performance of this developed immunoassay in food samples, different concentrations of AOZ standard were spiked into five different samples, then derived and measured by the signal-amplified GLFA. Uncontaminated samples were used as blank controls, and the assay results of them were negative similar to that of the PBS buffer. As shown in Fig. 7, the results of AOZ detection sensitivity in food samples demonstrate amazing agreement with those of the CPAOZ standard. Besides, the recovery rates were ranged from 87.0 to 120.1% (see ESM Table S2) by calculating the ratio between the actual found concentration and the original adding concentration of AOZ in food samples. Altogether, above results exhibited that complex food matrices have little or no influence on the assay performance, and the improved PLR system-based lateral flow biosensor has great potential for on-field detection of FZD residues in food samples.

Conclusion

In conclusion, a novel strategy for the construction of a GLFA sensing system for highly sensitive small molecule detection is described. Of particular note in this work is that a signal booster of Au-anti-Ab was introduced and dispensed successively with the detection probe of Au-Ab onto a same conjugate pad; then the system produced an attractive signal amplification effect in a minimalist manner by forming a powerful network structure and then accumulating numerous of GNPs on the T-line. Using this method, we have successfully detected AOZ with a sensitivity of 1 ng mL^{-1}. Meanwhile, we also confirm that this new GLFA biosensor possesses a good selectivity and practicability for AOZ analysis. More significantly, this approach will solve the conflict between enough signal intensity and limited Ab amount, as well as the contradiction of signal amplification and operational complexity in competitive format of GLFAs. Furthermore, it is fairly easy to generalize this strategy to detect a wide spectrum of small molecules by GLFA using different antibodies. By introducing other antibodies, this strategy poses great potential in generalizing detections of other small molecules by GLFA sensitively and simply.

Acknowledgements This work was supported by the National Natural Science Foundation of China (No. 21675127, 31501560), the New Century Excellent Talents in University (NCET-13-0483), and the Fundamental Research Funds for the Central Universities (2014YB093, 2452015257).

Compliance with ethical standards

Conflict of interest The authors declare that they have no conflict of interest.

References

1. Wang L, Cai J, Wang Y, Fang Q, Wang S, Cheng Q, et al. A bare-eye-based lateral flow immunoassay based on the use of gold nanoparticles for simultaneous detection of three pesticides. Microchim Acta. 2014;181(13–14):1565–72. https://doi.org/10.1007/s00604-014-1247-0.
2. Yao Y, Guo W, Zhang J, Wu Y, Fu W, Liu T, et al. Reverse fluorescence enhancement and colorimetric bimodal signal readout immunochromatography test strip for ultrasensitive large-scale screening and postoperative monitoring. ACS Appl Mater Interfaces. 2016;8(35):22963–70. https://doi.org/10.1021/acsami.6b08445.
3. Hu J, Jiang YZ, Wu LL, Wu Z, Bi Y, Wong G, et al. Dual-signal readout nanospheres for rapid point-of-care detection of Ebola virus glycoprotein. Anal Chem. 2017; https://doi.org/10.1021/acs.analchem.7b02222.
4. Chen Y, Sun J, Xianyu Y, Yin B, Niu Y, Wang S, et al. A dual-readout chemiluminescent-gold lateral flow test for multiplex and ultrasensitive detection of disease biomarkers in real samples. Nano. 2016;8(33):15205–12. https://doi.org/10.1039/c6nr04017a.
5. Yao L, Teng J, Zhu M, Zheng L, Zhong Y, Liu G, et al. MWCNTs based high sensitive lateral flow strip biosensor for rapid determination of aqueous mercury ions. Biosens Bioelectron. 2016;85:331–6. https://doi.org/10.1016/j.bios.2016.05.031.
6. Chen Y, Chen Q, Han M, Liu J, Zhao P, He L, et al. Near-infrared fluorescence-based multiplex lateral flow immunoassay for the simultaneous detection of four antibiotic residue families in milk. Biosens Bioelectron. 2016;79:430–4. https://doi.org/10.1016/j.bios.2015.12.062.
7. Yu L, Li P, Ding X, Zhang Q. Graphene oxide and carboxylated graphene oxide: viable two-dimensional nanolabels for lateral flow immunoassays. Talanta. 2017;165:167–75. https://doi.org/10.1016/j.talanta.2016.12.042.
8. Bahadır EB, Sezgintürk MK. Lateral flow assays: principles, designs and labels. TrAC Trends Anal Chem. 2016;82:286–306. https://doi.org/10.1016/j.trac.2016.06.006.
9. Duan H, Huang X, Shao Y, Zheng L, Guo L, Xiong Y. Size-dependent Immunochromatographic assay with quantum dot Nanobeads for sensitive and quantitative detection of ochratoxin A in corn. Anal Chem. 2017;89(13):7062–8. https://doi.org/10.1021/acs.analchem.7b00869.
10. Anfossi L, Baggiani C, Giovannoli C, D'Arco G, Giraudi G. Lateral-flow immunoassays for mycotoxins and phycotoxins: a review. Anal Bioanal Chem. 2013;405(2–3):467–80. https://doi.org/10.1007/s00216-012-6033-4.
11. Dzantiev BB, Byzova NA, Urusov AE, Zherdev AV. Immunochromatographic methods in food analysis. TrAC Trends Anal Chem. 2014;55:81–93. https://doi.org/10.1016/j.trac.2013.11.007.
12. Urusov AE, Petrakova AV, Zherdev AV, Dzantiev BB. "Multistage in one touch" design with a universal labelling conjugate for high-sensitive lateral flow immunoassays. Biosens Bioelectron. 2016;86:575–9. https://doi.org/10.1016/j.bios.2016.07.027.
13. Taranova NA, Urusov AE, Sadykhov EG, Zherdev AV, Dzantiev BB. Bifunctional gold nanoparticles as an agglomeration-enhancing tool for highly sensitive lateral flow tests: a case study with procalcitonin. Microchim Acta. 2017;184(10):4189–95. https://doi.org/10.1007/s00604-017-2355-4.
14. Wu Z, Fu Q, Yu S, Sheng L, Xu M, Yao C, et al. Pt@AuNPs integrated quantitative capillary-based biosensors for point-of-care testing application. Biosens Bioelectron. 2016;85:657–63. https://doi.org/10.1016/j.bios.2016.05.074.
15. Bu T, Huang Q, Yan L, Huang L, Zhang M, Yang Q, et al. Ultra technically-simple and sensitive detection for *Salmonella enteritidis* by immunochromatographic assay based on gold growth. Food Control. 2018;84:536–43. https://doi.org/10.1016/j.foodcont.2017.08.036.
16. Liao J-Y, Li H. Lateral flow immunodipstick for visual detection of aflatoxin B1 in food using immuno-nanoparticles composed of a silver core and a gold shell. Microchim Acta. 2010;171(3–4):289–95. https://doi.org/10.1007/s00604-010-0431-0.
17. Anfossi L, Di Nardo F, Giovannoli C, Passini C, Baggiani C. Increased sensitivity of lateral flow immunoassay for ochratoxin A through silver enhancement. Anal Bioanal Chem. 2013;405(30):9859–67. https://doi.org/10.1007/s00216-013-7428-6.
18. Mak WC, Beni V, Turner APF. Lateral-flow technology: from visual to instrumental. TrAC Trends Anal Chem. 2016;79:297–305. https://doi.org/10.1016/j.trac.2015.10.017.
19. Lu X, Liang X, Dong J, Fang Z, Zeng L. Lateral flow biosensor for multiplex detection of nitrofuran metabolites based on functionalized magnetic beads. Anal Bioanal Chem. 2016;408(24):6703–9. https://doi.org/10.1007/s00216-016-9787-2.
20. Xu YP, Liu LQ, Li QS, Peng CF, Chen W, Xu CL. Development of an immunochromatographic assay for rapid detection of 1-aminohydantoin in urine specimens. Biomed Chromatogr. 2009;23(3):308–14. https://doi.org/10.1002/bmc.1115.
21. Li S, Song J, Yang H, Cao B, Chang H, Deng A. An immunochromatographic assay for rapid and direct detection of 3-amino-5-morpholino-2-oxazolidone (AMOZ) in meat and feed samples. J Sci Food Agric. 2014;94(4):760–7. https://doi.org/10.1002/jsfa.6423.
22. Vass M, Hruska K, Franek M. Nitrofuran antibiotics: a review on the application, prohibition and residual analysis. Veterinarni Medicina. 2008;53(9):469–500.
23. Tang Y, Xu J, Wang W, Xiang J, Yang H. A sensitive immunochromatographic assay using colloidal gold–antibody probe for the rapid detection of semicarbazide in meat specimens. Eur Food Res Technol. 2010;232(1):9–16. https://doi.org/10.1007/s00217-010-1351-2.
24. Zhang D, Li P, Yang Y, Zhang Q, Zhang W, Xiao Z, et al. A high selective immunochromatographic assay for rapid detection of aflatoxin B(1). Talanta. 2011;85(1):736–42. https://doi.org/10.1016/j.talanta.2011.04.061.
25. Zhang D, Li P, Zhang Q, Zhang W. Ultrasensitive nanogold probe-based immunochromatographic assay for simultaneous detection of total aflatoxins in peanuts. Biosens Bioelectron. 2011;26(6):2877–82. https://doi.org/10.1016/j.bios.2010.11.031.
26. Di Nardo F, Baggiani C, Giovannoli C, Spano G, Anfossi L. Multicolor immunochromatographic strip test based on gold nanoparticles for the determination of aflatoxin B1 and fumonisins. Microchim Acta. 2017;184(5):1295–304. https://doi.org/10.1007/s00604-017-2121-7.
27. Gao H, Han J, Yang S, Wang Z, Wang L, Fu Z. Highly sensitive multianalyte immunochromatographic test strip for rapid chemiluminescent detection of ractopamine and salbutamol. Anal Chim Acta. 2014;839:91–6. https://doi.org/10.1016/j.aca.2014.05.024.

28. Zhang DH, Li PW, Zhang Q, Yang Y, Zhang W, Guan D, et al. Extract-free immunochromatographic assay for on-site tests of aflatoxin M-1 in milk. Anal Methods. 2012;4(10):3307–13. https://doi.org/10.1039/c2ay25205h.
29. Posthuma-Trumpie GA, Korf J, van Amerongen A. Lateral flow (immuno)assay: its strengths, weaknesses, opportunities and threats. A literature survey. Anal Bioanal Chem. 2009;393(2):569–82. https://doi.org/10.1007/s00216-008-2287-2.
30. Zhong Y, Chen Y, Yao L, Zhao D, Zheng L, Liu G, et al. Gold nanoparticles based lateral flow immunoassay with largely amplified sensitivity for rapid melamine screening. Microchim Acta. 2016;183(6):1989–94. https://doi.org/10.1007/s00604-016-1812-9.
31. Zhang MZ, Wang MZ, Chen ZL, Fang JH, Fang MM, Liu J, et al. Development of a colloidal gold-based lateral-flow immunoassay for the rapid simultaneous detection of clenbuterol and ractopamine in swine urine. Anal Bioanal Chem. 2009;395(8):2591–9. https://doi.org/10.1007/s00216-009-3181-2.
32. Tang Y, Xu X, Liu X, Huang X, Chen Y, Wang W, et al. Development of a lateral flow immunoassay (LFA) strip for the rapid detection of 1-aminohydantoin in meat samples. J Food Sci. 2011;76(6):T138–43. https://doi.org/10.1111/j.1750-3841.2011.02217.x.